Comparison of anti-scatter grids for digital imaging with use of a direct-conversion flat-panel detector

メタデータ	言語: eng
	出版者:
	公開日: 2017-10-03
	キーワード (Ja):
	キーワード (En):
	作成者:
	メールアドレス:
	所属:
URL	http://hdl.handle.net/2297/30544

Comparison of anti-scatter grids for digital imaging with use of a direct-conversion flat-panel detector

ABSTRACT

Our purpose in this study was to establish a selection standard for anti-scatter grids for a direct conversion flat-panel detector (FPD) system.   As indices for grid evaluation, we calculated the selectivity, Bucky factor, and the signal-to-noise ratio improvement factor (SIF) by measuring rates of scatter transmission, primary transmission, and total transmission (based on the digitally displayed measurement values of the FPD system), by using 4 acrylic phantoms of different thicknesses.   The results showed that the SIF was less than 1.0 when the phantom thickness was 5 cm.   When the phantom thickness was 25 cm and the grid ratio was 16:1, the SIF was 1.505 and 1.518 (maximum value) at 90 and 120 kV, respectively.   Compared with the grid ratio of 12:1, the SIF at the grid ratio 16:1 was improved by 6.1% at 90 kV, and by 7.0% at 120 kV.   In a direct-conversion FPD system, the grid ratio of 16:1 is considered adequate for eliminating the scattered-radiation effect when much scattered radiation is present, such as with a thick imaged object or a high X-ray tube voltage.

Keywords: Direct-conversion flat-panel detector・Anti-scatter grids・Signal-to-noise ratio improvement factor

1. INTRODUCTION

An important factor in image quality improvement in X-ray imaging is the elimination of scattered radiation, which would otherwise reduce the image contrast and affect the detectability of subtle signals [1, 2].

The anti-scatter grid is a well-known tool for eliminating scattered radiation, and we have been employing various types of anti-scatter grids depending on the imaged target region of the body [3-8].   Conventionally, the selection of an appropriate grid for X-ray imaging has been based on the calculated selectivity and Bucky factor, by measurement of the scatter transmission(T_s), primary transmission(T_p), and total transmission(T_t), according to Standard IEC60627 established by the International Electrotechnical Commission (IEC) [9]. It has been shown that digital processing can enhance subtle contrast, and that the only factor limiting such enhancement processing is noise.   The signal-to-noise ratio (SNR) is an appropriate physical value for indicating digital image quality.   For selection of grids in X-ray imaging, the signal-to-noise ratio improvement factor (SIF) indicates the degree of SNR improvement when grids are used[10-14].   A fluorescence meter is generally used for the measurement of scatter transmission, primary transmission, and total transmission, according to the IEC60627 standard [15]. However, this method is considered unsuitable for a direct-conversion flat panel detector (FPD) system because the X-rays are not converted into light; amorphous selenium (a-Se) is used as an X-ray converter, and each X-ray quantum is directly converted into an electric charge.

The digital value of an FPD system increases linearly in accordance with a radiation dose increase.   Therefore, for grid selection of a direct conversion FPD system, digital

values measured by the FPD system are used, instead of fluorescence values measured by a fluorometer.　It is desirable to calculate the selectivity, Bucky factor, and SIF by digitally measuring the scatter transmission, primary transmission, and total transmission.

　Our purpose in this study was to determine the optimum scattered X-ray elimination grid for a direct-conversion FPD system with a-Se, by digitally measuring the scatter transmission, primary transmission, and total transmission at 7 different grid ratios (4:1, 6:1, 8:1, 10:1, 12:1, 14:1, and 16:1) and by calculating the selectivity, Bucky factor, and SIF.

2.　METHODS

2-1. Equipment

The imaging apparatus used in our study was a direct-conversion FPD system (RADIOTEX Safire; Shimadzu Co., Kyoto, Japan; sensor film, a-Se; sensor film thickness, 1,000 μm; matrix size, 2,880 × 2,880; pixel pitch, 150 μm; output gradient, 14 bits).　The high voltage X-ray device was based on the inverter method, with use of an X-ray tube (CIRCLEX P-type 0.6/1.2 18DE&38 DE-85) with a focal spot diameter of 1.2 mm.　The anti-scatter grids used for measurement (Mitaya Co., Tokyo, Japan) had grid ratios of 4:1, 6:1, 8:1, 10:1, 12:1, 14:1, and 16:1, each with a grid density of 60 units/cm (Table 1).　An aluminum inter-spacer was used, and the focal distance was 120 cm.　The direct-conversion FPD system in the present study eliminated scattered radiation by a moving grid.

2-2. X-ray conditions for measurement and phantom thickness

The X-ray tube voltage was set at 60, 90, or 120 kV, considering the conditions for clinical X-ray imaging with anti-scatter grids.   Acrylic phantoms of 5, 15, 20, and 25 cm thickness were used, although the combination of a 60 kV tube voltage and a 25 cm-thick acrylic phantom was disregarded from our measurement because it was irrelevant for clinical practice.

2-3. Total transmission measurement

Figure 1 shows the configuration for total transmission measurement, designed according to the IEC60627 standard.   The radiation field was 30×30 cm, and the outside of the radiation field was covered with a lead collimator.   The detector region of the FPD system was 10 mm in diameter, and its outside was covered with a lead collimator.   The incident point of X-rays was set in the center of the FPD, and the X-rays entered perpendicularly to the FPD. Measurement were made at the center of the panel, and the measured size was 10mm in diameter.

The total transmission rate is expressed by the following equation :

$$Tt = \frac{It'}{It}, \qquad (1)$$

where It' is the digital value with anti-scatter grids, and It is the digital value without the grids.

2-4. Scatter transmission measurement

Figure 2 shows the configuration for measurement of the scatter transmission, which was designed according to the IEC60627 standard.   The radiation field was 30 cm × 30 cm, and the outside of the radiation field was covered with a lead collimator.   The detector region of the FPD system was 10 mm in diameter, and its outside was covered with a lead collimator.   In order to cover the detector region evenly, a lead disk 20 mm

in diameter was placed on the phantom.　The incident point of X-rays was set in the center of the FPD, and the x-rays entered perpendicularly to the FPD.　Measurement were made at the center of the panel, and the measured size was 10mm in diameter.

　The scatter transmission rate is expressed by the following equation :

$$Ts = \frac{Is'}{Is}, \qquad (2)$$

where Is' is the digital value with grid, and Is is the digital value without grid.

2-5. Primary transmission measurement

Figure 3 shows the configuration for primary transmission measurement, which was designed according to the IEC60627 standard.　The radiation field was 10 mm in diameter, and the outside of the detector field was covered with a lead collimator. The incident point of X-rays was set in the center of the FPD, and the X-rays entered perpendicularly to the FPD.　Measurement were made at the center of the panel, and the measured size was 10mm in diameter.

　The primary transmission rate is expressed by the following equation:

$$Tp = \frac{Ip'}{Ip}, \qquad (3)$$

Where Ip' is the digital value with grid, and Ip is the digital value without grid.

2-6. Selectivity (calculation method for Bucky factor)

Selectivity is the ratio of primary transmission to scatter transmission.　A larger selectivity is better, because the selectivity shows relative improvement in the ratio of primary X-rays to scattered X-rays.　The Bucky factor is the reciprocal of the total transmission rate; thus, a smaller Bucky factor is better.

$$Selectivity(\Sigma) \qquad : \Sigma = \frac{Tp}{Ts}, \qquad (4)$$

$$Bucky\ Factor（B） \quad : B = \frac{1}{Tt}, \qquad (5)$$

2-7. Signal-to-noise ratio improvement factor calculation method

The signal (ΔI) and contrast (C) of the detailed (minute) structure of an imaged object with low contrast are expressed by the following equations:

$$\Delta I = \Delta\mu \cdot dp \cdot I, \qquad (6)$$

$$C = \frac{\Delta I}{I} = \Delta\mu \cdot dp, \qquad (7)$$

where $\Delta\mu$ is the linear attenuation coefficient and dp is depth. The signal (ΔI) is expressed as the difference in the mean quantum number ($\Delta\bar{N}$), and is shown by the following equation when only quantum noise to the SNR is considered:

$$SNR = \frac{\Delta\bar{N}}{\sqrt{\bar{N}}} = \Delta\mu \cdot d \cdot \sqrt{\bar{N}}, \qquad (8)$$

The reason for the signal increases proportionally to the number of quantum ($\bar{N}$) which pass through the imaged object, and quantum noise follows a Poisson distribution, so that it is proportional to the square root of *N*. The effect of scattered X-rays on the SNR can be evaluated by the scatter degradation factor (SDF). The SDF without use of grids (SDF$_0$) and that with grids (SDF$_g$) are expressed by the following equations:

$$SDF_0 = \frac{1}{1+\frac{Is}{Ip}}, \qquad (9)$$

$$SDF_g = \frac{1}{1+\frac{Is \cdot Ts}{Ip \cdot Tp}}. \qquad (10)$$

Digital images can be enhanced to show subtle differences in contrast by image-processing techniques. The level of detail of a low-contrast object which can be displayed is determined by the amount of noise. The image quality of digital images is evaluated by use of the SNR. Thus, the effect of anti-scatter grids on digital images can be evaluated by the improvements in the SNR and SIF.

The SIF with use of grids is expressed by the following equation, supposing that the SNR without grids is SNRo and that with grids is SNRg:

$$SIF = \frac{SNR_g}{SNR_0}, \qquad (11)$$

The SIF with use of grids can be expressed by the following equations, using Cp as the contrast that would be obtained if there were no scattered x-rays:

$$SNR_0 = Cp \cdot SDF_0 \cdot \sqrt{Ip + Is}, \qquad (12)$$

$$SNR_g = Cp \cdot SDF_g \cdot \sqrt{Tp \cdot Ip + Ts \cdot Is}, \qquad (13)$$

$$SIF = \frac{SNR_g}{SNR_0} = \frac{Tp}{Tt} \cdot \frac{\sqrt{It'}}{\sqrt{It}} = \frac{Tp}{Tt} \cdot \sqrt{Tt}, \qquad (14)$$

3. RESULTS

Table 2 shows the primary transmission, scatter transmission, and total transmission measured with seven different grid ratios.   Table 3 shows the SIF, Bucky factor (B), and selectivity ($\sum$), which are calculated from Table 2.

As noted in Table 2, the higher the grid ratio, the less Ts, Tp, and Tt, for all acrylic phantom thicknesses and tube voltages tested.   At the same phantom thickness and grid ratio, a higher tube voltage gave greater Ts, Tp, and Tt.

3-1. Signal-to-noise ratio improvement factor

As noted in Table 3, when an acrylic phantom of 5 cm thickness measured, the SIF was less than 1.0, irrespective of the tube voltages and grid ratios (for all tube voltages and grid ratios tested).   When we used an acrylic phantom of 15 cm thickness, the SIF was less than 1.0 at the grid ratio of 4:1.   When the tube voltage was 60 kV, the SIF at grid ratio 16:1 improved by 11.9% compared with that at grid ratios 4:1.   When the tube voltage was 90 kV, the SIF at grid ratio 16:1 improved by 35.7% and 11.6% compared with those at grid ratios 4:1 and 12:1, respectively.   Using for an acrylic phantom of 25 cm thickness and a tube voltage of 90 kV, the SIF at grid ratio 16:1 improved by 24.2 and 6.1% compared with those at grid ratios 4:1 and 12:1, respectively.   When the tube

8

voltage was 120 kV, the SIF at grid ratio 16:1 improved by 31.1 and 7.0% compared with those at grid ratios 4:1 and 12:1, respectively.

3-2. Selectivity

When we used an acrylic phantom of 5 cm thickness, the selectivity at tube voltage 60 kV and grid ratio 16:1 improved by approximately 12 times compared with that at grid ratio 4:1.   The selectivity at tube voltage 90 kV and grid ratio 16:1 improved by approximately 5.0 times compared with that at grid ratio 4:1.   The selectivity at tube voltage 120 kV and grid ratio 16:1 improved by approximately 4.2 times compared with that at grid ratio 4:1.

For an acrylic phantom of 25 cm thickness, the selectivity at tube voltage 90 kV and grid ratio 16:1 improved by approximately 4.5 times compared with that at grid ratio 4:1. The selectivity at tube voltage 120 kV and grid ratio 16:1 improved by approximately 4.2 times compared with that at grid ratio 4:1.

3-3. Bucky Factor

When we used an acrylic phantom of 5 cm thickness, the Bucky factor at tube voltage 60 kV and grid ratio 16:1 improved by approximately 1.6 times compared with that at grid ratio 4:1.   The Bucky factor at tube voltage 90 kV and grid ratio 16:1 improved by approximately 1.7 times compared with that at grid ratio 4:1.   The Bucky factor at tube voltage 120 kV and grid ratio 16:1 improved by approximately 1.7 times compared with that at grid ratio 4:1.

For an acrylic phantom of 25 cm thickness, the Bucky factor at tube voltage 90 kV and grid ratio 16:1 improved by approximately 2.8 times compared with that at grid ratio 4:1.   The Bucky factor at tube voltage 120 kV and grid ratio 16:1 improved by approximately 3.1 times compared with that at grid ratio 4:1.

4. DISCUSSION

In the present study, we calculated the selectivity, Bucky factor, and SIF by measuring the rates of scatter transmission, primary transmission, and total transmission using anti-scatter grids of a direct-conversion FPD system, indicating the selection criteria of anti-scatter grids for a direct-conversion FPD system with a-Se.

We obtained the scatter transmission, primary transmission, and total transmission measured with a direct-conversion FPD system, as shown in Table 2. Our results almost agreed with the report of Ishikawa et al. [9], who used a fluorescence meter and a detector; namely, the value of scatter transmission, primary transmission, and total transmission decreased in accordance with an increase in the grid ratio. The slight differences between their results and our results are assumed to be due to the difference in the measurement device used for scatter transmission and the differences in the grid structure (fixed type v.s. moving type), although this could not be determined in the present study.

We also obtained the SIF, Bucky factor, and selectivity, as shown in Table 3. The Bucky factor and selectivity increased in accordance with the increase in the grid ratio, which agreed with the report of Ishikawa et al. [9]. Although a good grid is defined by the combination of a small Bucky factor and large selectivity, the larger the selectivity, the larger the Bucky factor, in general. Anti-scatter grids with large selectivity should be used when there are many scattered X-rays. However, this increases the radiation exposure of patients due to the increased Bucky factor. Therefore, neither the Bucky factor nor the selectivity alone is appropriate for considering the selection of grids in digital imaging. For analogue images, a grid is selected based on the contrast improvement factor (CIF), which is the ratio of primary transmission to total transmission, whereas for digital images, the CIF is not a suitable indicator for grid selection because the contrast can be arbitrarily adjusted by image-processing techniques after raw image data are obtained. Therefore, the SIF which we calculated as

an index for grid selection is considered to be very useful for a digital imaging system.

The SIF was less than 1.0 irrespective of the X-ray tube voltage, when we used an acrylic plate of 5 cm thickness, indicating no SNR improvement with the use of anti-scatter grids. The following equation reported by Chan et al. [14] shows the SNR by primary transmission and contend of scattered X-rays (S):

$$SNR \propto \sqrt{(1-S)Tp}, \qquad (15)$$

We consider that the reason for the small amount of scattered X-rays with an acrylic phantom of 5 cm thickness without use of grids is that there was a great reduction of primary transmission compared with that when grids are used.

Also, the SIF was less than 1.0 at tube voltages of 60, 90, and 120 kV when we used an acrylic plate of 15 cm thickness and a grid ratio of 4:1. The cause is considered to be the fact that the 4:1 ratio grid had a smaller scattered X-ray elimination effect.

Court et al. [11] reported the grid selection standard for a direct-conversion FPD system. Their results had an SIF of less than 1.0 at grid ratios of 4:1, 8:1, and 10:1 with use of a phantom of 15 cm thickness and an indirect-conversion FPD system (CXDI-31, Canon Inc., Tokyo, Japan), but their focal distance was slightly different from ours. The direct-conversion FPD in the present study had a sufficient scattered X-ray elimination effect even at grid ratios of 8:1 and 10:1; thus, it can be considered to have yielded SIFs of more than 1.0.

In the present study, we used aluminum as spacer material for the grids. The SIF is proportional to the primary transmission, according to the SIF Eq. 14. If the material of the spacer is changed from aluminum to another material with a lower atomic number, such as carbon or wood, images with better SNR would be obtained at the same grid ratio.

In the present study, the size of the radiation field for our measurements of scatter transmission and total transmission was 30 cm×30 cm, which conformed to the IEC60627 standard. Because the volume of scattered X-rays depends on the size of the radiation field, further study with different radiation field sizes is necessary. Although more data with different direct-conversion FPD systems are desirable, we believe that

the results of the present study can be used for selection of anti-scatter grids for direct-conversion FPD systems.

5. CONCLUSION

The SIF, selectivity and Bucky Factor were calculated using the physical characteristic values of anti-scatter grids, based on the digitally measured physical characteristic values of a direct-conversion FPD system.   When an object imaged using the direct-conversion FPD is thick, the grid ratio will be higher than that of conventionally used anti-scatter grids; thus, grids of a high scatter transmission rate should be used.   In future studies, determination of the optimum grid for each radiation field by adjusting of the size of the radiation field is desirable.

References

1. Niklason LT, Sorenson JA, Nelson JA. Scattered radiation in chest radiography. Med Phys. 1981;8:677-81.

2. Fetterly KA, Schueler BA. Physical evaluation of prototype high-performance anti-scatter grids: potential for improved digital radiographic image quality. Phys Med Biol. 2009;54:37-42.

3. Sandborg M, Dance DR, Carlsson GA, Persliden J. Monte Carlo study of grid performance in diagnostic radiology: task dependent optimization for screen-film imaging. Br J Radiol. 1994;67:76-85.

4. Sandborg M, Dance DR, Carlsson GA, Persliden J. Monte Carlo study of grid performance in diagnostic radiology: factors which affect the selection of tube potential and grid ratio. Br J Radiol. 1993;66:1164-76.

5. Sandborg M, Dance DR, Carlsson GA, Persliden J. Selection of anti-scatter grids for different imaging tasks: the advantage of low atomic number cover and interspace materials. Br J Radiol. 1993;66:1151-63.

6. McVey G, Sandborg M, Dance DR, Alm Carlsson G. A study and optimization of lumbar spine X-ray imaging systems. Br J Radiol. 2003;76:177-88.

7. Chan HP, Doi K. The validity of Monte Carlo simulation in studies of scattered radiation in diagnostic radiology. Phys Med Biol. 1983;28:109-29.

8. Chan HP, Higashida Y, Doi K. Performance of antiscatter grids in diagnostic radiology: experimental measurements and Monte Carlo simulation studies. Med Phys. 1985;12:449-54.

9. Ishikawa M, Ide T, Asano H, Sagawa Z, Miyake H, Kamishima Y, Negishi T. Physical characteristics of anti-scatter grids according to old and new JIS standards. Nippon Hoshasen Gijutsu Gakkai Zasshi. 2004;60:1123-31. *in Japanese.*

10. Sandborg M, Carlsson G A. Influence of X-ray energy spectrum, contrasting detail

and detector on the signal-to-noise ratio (SNR) and detective quantum efficiency (DQE) in projection radiography. Phys Med Biol. 1992; 37:1245-1263

11. Court L, Yamazaki T. Technical note: a comparison of antiscatter grids for digital radiography.Br J Radiol. 2004;77:950-2.

12. Fetterly KA, Schueler BA. Experimental evaluation of fiber-interspaced antiscatter grids for large patient imaging with digital x-ray systems. Phys Med Biol. 2007 21;52:4863-80.

13. Neitzel U, Maack I, Günther-Kohfahl S. Image quality of a digital chest radiography system based on a selenium detector. Med Phys.1994;21:509-16

14. Chan HP, Lam KL, Wu YZ. Studies of performance of antiscatter grids in digital radiography: effect on signal-to-noise ratio. Med Phys. 1990;17:655-64.

15. IEC61267: Medical diagnostic x-ray equipment-radiation conditions for use in the determination of characteristics.1994

FDD: Focus-detector distance

X-ray tube

Lead collimator

FDD:1000mm

Field size 30cm × 30cm

Lead collimator

Lead collimator 10mmφ

Top board

Grid

FPD panel

Fig. 1 Configuration for total transmission measurement

FDD: Focus-detector distance

X-ray tube

Lead collimator

FDD:1000mm

Field size 30cm × 30cm

20mmφ

Lead collimator

Acrylic phantom

Lead collimator 10mmφ

Top board

Grid

FPD panel
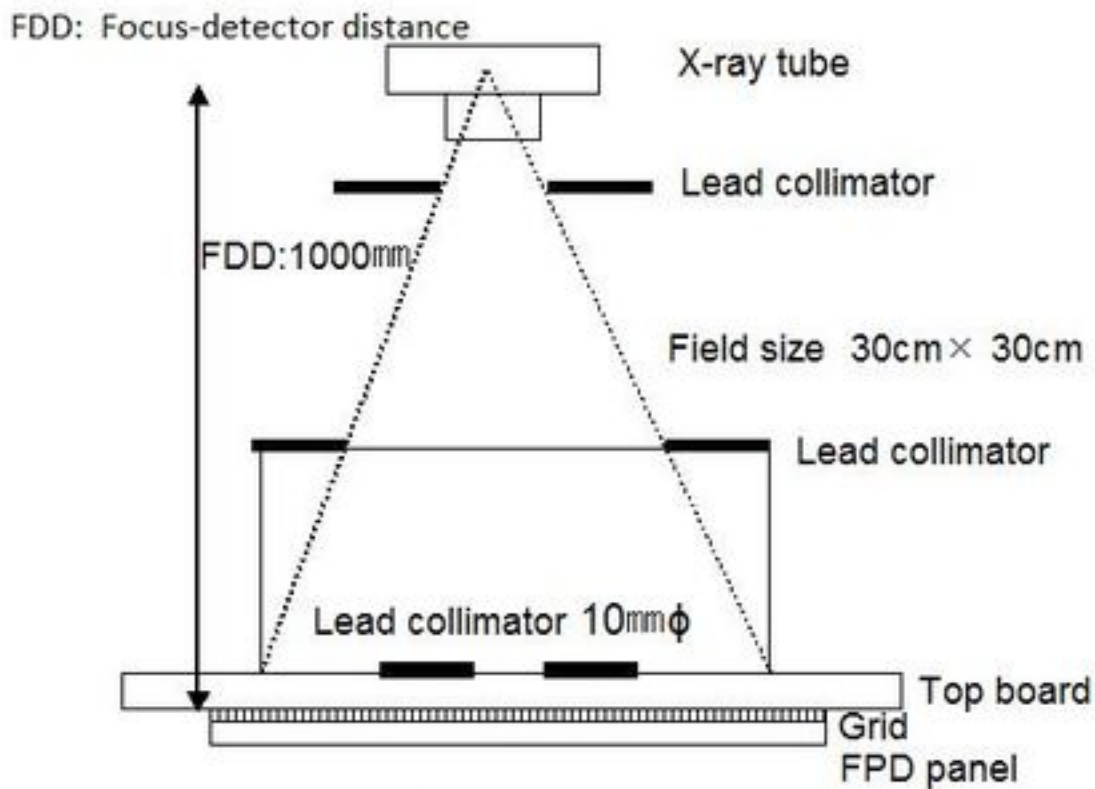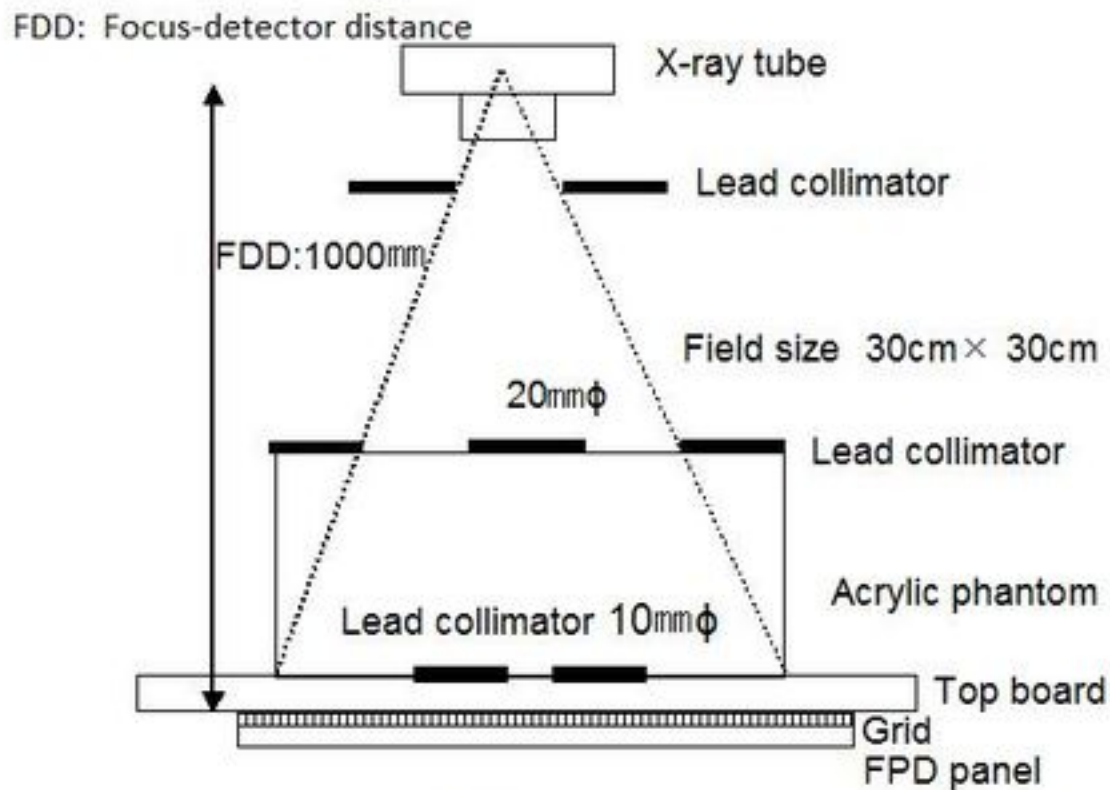
Fig. 2 Configuration for scatter transmission measurement

FDD: Focus-detector distance

X-ray tube

Lead collimator

Acrylic phantom

Lead collimator

FDD:1000mm

10mmφ

Lead collimator

Top board

Grid

FPD panel
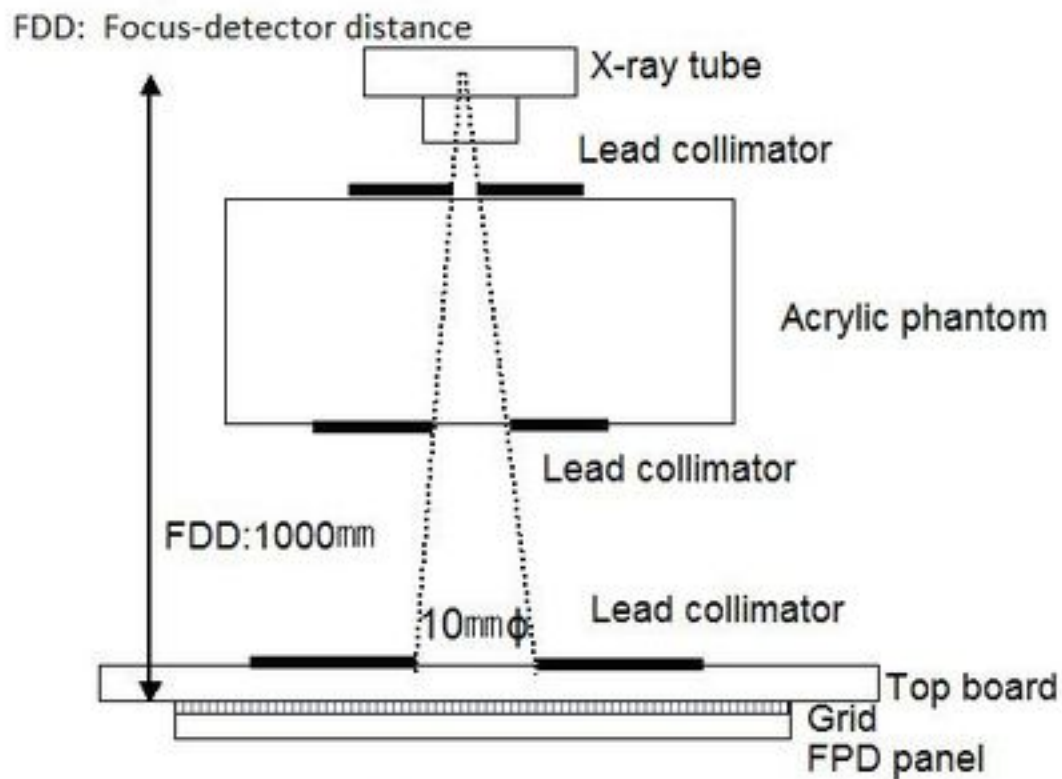
Fig. 3 Configuration for total transmission measurement

Table 1 Structures of 7 anti-scatter grids

Grid ratios (r)	Strip density (N)(cm^{-1})	Strip width (d) (μm)	Interspace width (D) (μm)	Strip height (h) (μm)	Cover thickness (top + bottom) (2t) (μm)	Protective cover	Total thickness (mm)
4	60	49	120	480	300	Aluminum	0.88
6	60	49	120	720	300	Aluminum	1.12
8	60	49	120	960	300	Aluminum	1.36
10	60	49	120	1200	300	Aluminum	1.60
12	60	49	120	1440	300	Aluminum	1.84
14	60	49	120	1680	300	Aluminum	2.08
16	60	49	120	1920	300	Aluminum	2.32

Data are shown as parameters of commercially available grids.

The grids are specified by the strip density, N; strip width, d; interspace width, D; grid ratio, r; and cover thickness, t.

The grid ratio is the ratio of the strip height (h) to the interspace width (D).

The thickness of the coating (top and bottom) was 0.05 μm.

Table 2 Data of measured physical characteristics (Ts,Tp,and Tt)

Thickness of acrylic plate (cm)	Grid ratio (r)	X-ray tube voltage								
		60 kV			90 kV			120 kV		
		Ts	Tp	Tt	Ts	Tp	Tt	Ts	Tp	Tt
5 cm	4:1	0.172	0.633	0.472	0.274	0.637	0.520	0.332	0.692	0.537
	6:1	0.085	0.599	0.410	0.175	0.607	0.435	0.226	0.660	0.471
	8:1	0.053	0.589	0.376	0.121	0.582	0.401	0.178	0.648	0.407
	10:1	0.038	0.567	0.364	0.094	0.571	0.369	0.128	0.614	0.394
	12:1	0.028	0.517	0.328	0.066	0.542	0.344	0.094	0.589	0.350
	14:1	0.020	0.502	0.318	0.051	0.532	0.330	0.082	0.574	0.344
	16:1	0.011	0.487	0.292	0.045	0.517	0.302	0.062	0.545	0.316
15 cm	4:1	0.202	0.603	0.368	0.322	0.646	0.430	0.356	0.669	0.455
	6:1	0.105	0.579	0.281	0.195	0.630	0.340	0.230	0.653	0.369
	8:1	0.067	0.546	0.245	0.134	0.607	0.288	0.167	0.633	0.305
	10:1	0.051	0.516	0.218	0.097	0.580	0.262	0.129	0.594	0.268
	12:1	0.035	0.484	0.209	0.080	0.564	0.221	0.100	0.580	0.229
	14:1	0.032	0.465	0.185	0.058	0.548	0.210	0.075	0.564	0.218
	16:1	0.018	0.457	0.169	0.046	0.534	0.159	0.058	0.546	0.193
20 cm	4:1				0.321	0.663	0.393	0.366	0.697	0.435
	6:1				0.194	0.623	0.310	0.245	0.663	0.328
	8:1				0.132	0.595	0.248	0.177	0.634	0.268
	10:1				0.105	0.564	0.214	0.128	0.619	0.232
	12:1				0.078	0.533	0.197	0.100	0.600	0.200
	14:1				0.060	0.525	0.163	0.080	0.576	0.184
	16:1				0.050	0.506	0.154	0.064	0.560	0.165
25 cm	4:1				0.303	0.730	0.363	0.366	0.737	0.405
	6:1				0.185	0.670	0.267	0.244	0.695	0.295
	8:1				0.132	0.641	0.227	0.178	0.666	0.235
	10:1				0.097	0.592	0.189	0.132	0.619	0.205
	12:1				0.075	0.562	0.157	0.104	0.582	0.168
	14:1				0.058	0.538	0.128	0.078	0.555	0.138
	16:1				0.049	0.538	0.128	0.065	0.551	0.131

Ts scatter transmission, *Tp* primary transmission, *Tt* total transmission

Table 3   Results of calculated physical characteristics (SIF, Bucky factor, and Σ)

Thickness of Acrylic plate(cm)	Grid ratio(r)	X-ray tube voltage								
		60 kV			90 kV			120 kV		
		SIF	B	Σ	SIF	B	Σ	SIF	B	Σ
	4:1	0.921	2.118	3.689	0.884	1.923	2.326	0.944	1.862	2.086
	6:1	0.935	2.436	7.024	0.920	2.301	3.476	0.961	2.123	2.922
	8:1	0.962	2.663	11.085	0.919	2.494	4.821	0.943	2.457	3.645
5 cm	10:1	0.939	2.745	14.868	0.940	2.708	6.087	0.978	2.537	4.808
	12:1	0.903	3.047	18.418	0.923	2.905	8.153	0.966	2.860	6.237
	14:1	0.890	3.141	25.044	0.925	3.027	10.378	0.980	2.909	7.025
	16:1	0.901	3.426	44.131	0.941	3.314	11.572	0.969	3.162	8.828
	4:1	0.995	2.721	2.983	0.985	2.326	2.007	0.993	2.199	1.883
	6:1	1.092	3.554	5.523	1.079	2.937	3.235	1.074	2.707	2.843
	8:1	1.104	4.087	8.170	1.132	3.474	4.529	1.146	3.278	3.792
15 cm	10:1	1.105	4.585	10.163	1.134	3.819	5.982	1.146	3.726	4.605
	12:1	1.060	4.796	13.957	1.198	4.516	7.047	1.214	4.375	5.814
	14:1	1.083	5.418	14.466	1.197	4.769	9.438	1.207	4.581	7.517
	16:1	1.113	5.931	25.731	1.337	6.271	11.601	1.244	5.180	9.465
	4:1				1.057	2.543	2.064	1.057	2.300	1.904
	6:1				1.119	3.229	3.214	1.158	3.052	2.707
	8:1				1.195	4.031	4.504	1.226	3.735	3.584
20 cm	10:1				1.218	5.673	5.391	1.286	4.301	4.835
	12:1				1.201	5.074	6.827	1.341	4.992	6.008
	14:1				1.300	6.135	8.796	1.342	5.429	7.180
	16:1				1.289	6.501	10.180	1.378	6.065	8.739
	4:1				1.212	2.758	2.406	1.158	2.469	2.015
	6:1				1.297	3.474	3.626	1.280	3.388	2.850
	8:1				1.345	4.411	4.859	1.373	4.255	3.742
25 cm	10:1				1.363	5.303	6.114	1.366	4.867	4.701
	12:1				1.418	6.367	7.478	1.419	5.941	5.619
	14:1				1.501	7.784	9.326	1.494	7.243	7.116
	16:1				1.505	7.834	10.995	1.518	7.605	8.439

SIF signal-to-noise ratio improvement factor, *B* Bucky factor, Σ selectivity